A Compact Mass-producible E-band Bandpass Filter Based on Multi-layer Waveguide Technology

Abbas Vosoogh[1], Astrid Algaba Brazález[2], Yinggang Li[2], and Zhongxia Simon He[3]
[1]Metasum AB, Gothenburg, Sweden, abbas.vosoogh@metasum.se
[2]Ericsson Research, Ericsson AB, Gothenburg, Sweden, astrid.algaba.brazalez@ericsson.com
[3]Department of Microtechnology and Nanoscience, Chalmers University of Technology, Gothenburg, Sweden

***Abstract*—This paper presents the design, implementation and experimental validation of a bandpass filter for high-data rate point-to-point link applications at E-band. The proposed design is developed in multilayer waveguide (MLW) technology, where an air-filled waveguide transmission line is formed by stacking several unconnected thin metal plates. Our MLW bandpass filter is designed by combining low-pass and high-pass filtering structures, and consists of 19 separate metal layers. An array of glide-symmetric holes, which act as an electromagnetic band gap (EBG) structure, are used to prevent any possible field leakage due to the air gaps between the layers. The fabricated filter provides a bandpass from 71.5 to 76 GHz with measured return loss better than 15 dB, and insertion loss better than 1.3 dB. The investigation of the potential for mass-production, as well as an evaluation of the MLW filter response for temperature variations from -30°C to +70°C are discussed in this paper. The measured results show that the MLW filter has a center frequency thermal stability parameter of 9.3 ppm/°C, and center frequency drift of less than 0.12% over the whole temperature range. These results confirm the advantages of MLW technology for implementing ultra-compact bandpass filters showing low loss and potential for being mass-produced at millimeter-wave frequencies.**

***Index Terms*—Backhaul, bandpass filter, electromagnetic bandgap (EBG), glide symmetry, millimeter wave, multilayer waveguide (MLW), thermal.**

I. Introduction

Ultra-high data rate backhaul point-to-point wireless links constitutes a flexible and cost-effective alternative to optic fiber systems. One of the frequency bands of interest for wireless backhaul is the E-band, which covers the ranges 71-76 and 81-86 GHz [1]. This particular interval of frequencies can provide multi-Gbit/s data transfer [2], as well as low atmospheric attenuation of approximately 0.4 dB/km [3]. Filters constitute an essential passive component in the RF chain of E-band point-to-point wireless link modules. As the operating frequency increases, the required manufacturing and assembly tolerances become very strict. In high frequencies, even a small discrepancy with respect to the nominal design dimensions and structure alignment can degrade the component performance. This is especially critical in the case of filters operating at millimeter-wave frequency bands and beyond, where tolerances can cause bandwidth shift, leakage loss and degradation of the Q-factor.

An efficient implementation of high-quality and competitive filter products starts by taking into account some type of design compensation already in the numerical analysis stage to counterbalance manufacturing and assembly effects. This implies a cost in terms of design and simulation time. On the other hand, using more precise fabrication techniques might mitigate the tolerance issue and relax the simulation time, but it increases manufacturing cost. It is, thereby, needed a trade-off between design/simulation time, and fabrication/assembly cost to implement high-performance and cost-effective filter products [4]–[6] with potential to be mass-produced. Moreover, filters with stable response to temperature variations [7], [8] are of interest to be integrated into millimeter-wave backhaul wireless modules, which usually operate in outdoor environments and are exposed to thermal changes.

Chosing a suitable hardware technology to implement filters that fulfill the strict requirements at millimeter-wave frequencies is a critical task. The use of hollow waveguides offers the advantages of providing high Q-factors and power handling capacity, as well as low loss performance. However, waveguide components are bulky, complex to be integrated with the remaining circuitry of the RF system and costly to realize at large scale production due to the precise fabrication method.

Alternative manufacturing methods to the expensive standard Computer Numerical Control (CNC) milling technique, like additive manufacturing (3-D printing) [9] and micromachining technology [10], have been recently introduced as potential aproaches to mass-produce highly-efficient waveguide components. An E-band waveguide filter realized by difussion bonding of laminated thin metal layers is presented in [11]. Difussion bonding technique provides accurate prototyping and precise alignment of split-blocks for implementing high-performance waveguide components. However, it does not really constitute a cost-effective solution for large scale production. Gap waveguide [12] is a promising low loss technology that can replace hollow waveguides. It shows the advantages of high integrability and assembly simplicity since no electrical contact between the building blocks is required. This is demonstrated in [13] where a complete compact integrated full-duplex gap waveguide front-end is proposed and validated. However, the pin texture used as electromagnetic bandgap (EBG) structure in gap waveguides are more complex and challenging to manufacture when moving upwards in frequency. Another option could be to use substrate integrated waveguide (SIW) [14], [15], which is a planar low-profile transmission line that preserves the electromagnetic properties of standard waveguides and can be fabricated with cost-

effective methods. The main drawback of SIW is the inherent higher insertion loss compared to hollow waveguides due to the employed substrate material.

A novel air-filled waveguide made by stacking multiple unconnected thin metal layers and known as multilayer waveguide (MLW), has been proposed and experimentally evaluated at D-band in [16]. The EBG unit cells on each thin metal layer with glide-symmetric configuration, suppress all possible leakage of fields, which simplifies the assembly process. In [17], a similar approach to implement waveguide components using glide-symmetric EBG holey structures in split-block configuration was proposed.

This paper presents the design, numerical simulations and experimental validation of a very compact and robust E-band bandpass filter (BPF) implemented in MLW technology. The viability of mass-production for future commercialization of MLW components is also discussed in this work. Furthermore, taking into account the relevance of the performance of filters when operating at different thermal scenarios, an experimental evaluation of the temperature dependence of the proposed MLW filter has been described as well.

II. MLW BANDPASS FILTER DESIGN

The first step towards the implementation of our proposed MLW filter is to design numerically an E-band filter following the theoretical approach described in [18]. In the following subsections, the design procedure is explained and simulation results are presented.

A. Basic bandpass filter

The design of the BPF is based on combining the response of low-pass and high-pass waveguide filtering structures. This configuration provides a more compact size, lower insertion loss and less tolerance sensitivity than waveguide cavity filters as the reported ones in [11], [13].

Fig. 1 shows the geometry of the proposed BPF, which consists of 19 sections. Narrow slots with thickness of 0.2 mm (t_1) provide high-pass filter response, whereas the other sections with thickness of 0.4 mm (t_2) are used for impedance matching and achieving low-pass filter response. The proposed filter has a symmetric configuration, where half of the sections are identical. The high-pass filter functionality is achieved by

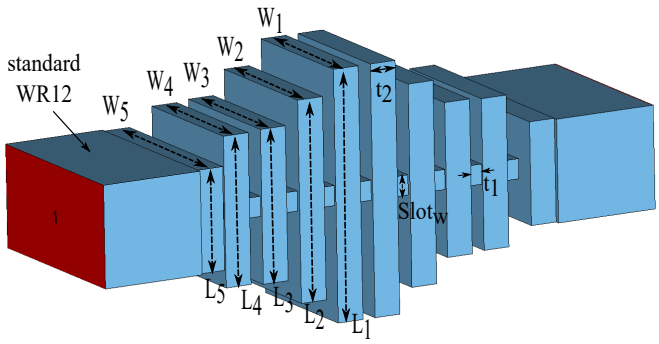

Fig. 1. Configuration of the proposed bandpass filter.

TABLE I
DIMENSIONS OF THE DESIGNED BANDPASS FILTER (REFERS TO FIG. 1)

Parameter	Value (mm)	Parameter	Value (mm)
L_1	3.8	W_1	2.24
L_2	3	W_2	2.28
L_3	2.3	W_3	2.23
L_4	2.27	W_4	2.21
L_5	1.55	W_5	2.9
t_1	0.2	t_2	0.4
$slot_L$	2.15	$slot_W$	0.3

the cutoff of the fundamental TE_{10} mode of a rectangular waveguide. The length of the coupling slots ($Slot_L$) is selected using the formula below:

$$slot_L = \frac{c_0}{2 \cdot f_0}. \quad (1)$$

where c_0 is the speed of light and f_0 should be selected smaller than the lower frequency in the desired bandpass (71 GHz).

In order to achieve a low-pass filtering response, the attenuation of the upper stopband is obtained by using corrugation sections of different heights L_i with length of λ_g, as it is thoroughly described in [18]. The upper frequency in the passband response and the rejection in the return loss are determined by the low-pass structure with longest height L_1. After combining the high-pass and low-pass filtering configurations, the structure shown in Fig. 1 has been optimized using CST Microwave Studio. The final optimized parameters of the designed BPF are presented in Table. I. The corresponding simulation results of the S-parameters are shown in Fig. 2. It is worthy to mention that we have considered a fixed thickness for the high-pass (t_1) and low-pass (t_2) sections in the designed procedure. This simplifies the fabrication of the filter by using thin metal sheets as explained in the next subsection.

B. Packaged BPF using MLW

After implementing the BPF design, the next step is to realize the filter in MLW technology. By doing this, we

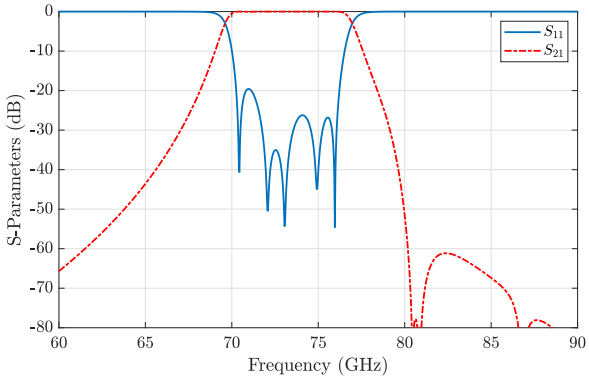

Fig. 2. Simulated performance of the designed BPF with basic waveguide topology.

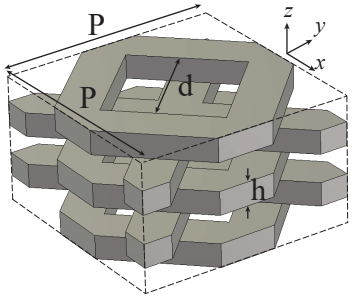

Fig. 3. Configuration of the unit cell with diamond-shaped holes consisting of five metallic layers. ($P = 4$ mm, $d = 1.8$ mm, and $h = 0.4$ mm)

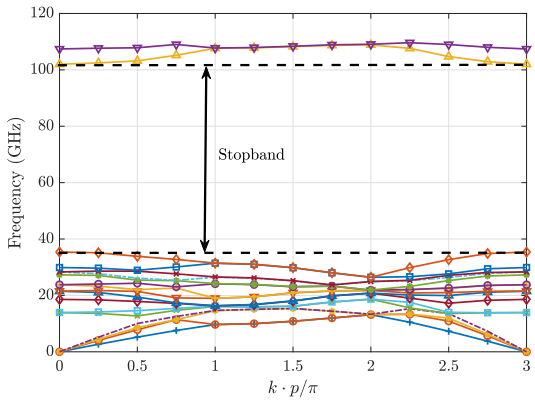

Fig. 4. Dispersion diagram for the infinite periodic unit cell with 5 metallic layers (refers to Fig. 3)

simplify the manufacturing and assembly process, as well as obtain a very compact filter profile.

The waveguide structure is built by stacking unconnected metal layers of thickness of 0.2 mm and 0.4 mm. These layers are separated by an air-gap, that can be between 0-20 μm with a negligible performance degradation. By adding an EBG pattern around the waveguide openings of each layer, any possible leakage of fields is avoided. The EBG structure is made by means of glide-symmetric diamond-shaped all-through holes unit cells. Fig. 3 shows the geometry of the glide-symmetric diamond-shaped holes unit cell consisting of 5 metal layers separated by a small gap (10μm). The corresponding dispersion diagram of this unit cell has been numerically calculated by using CST Eigenmode solver, and is depicted in Fig. 4. As can be observed, the unit cell provides a stopband over the frequency band from 40 to 100 GHz. Therefore, all unwanted waves are suppressed within that frequency band. It should be noted that the stopband of the proposed unit cell would be the same even if we increase the number of layers.

We integrate the glide-symmetric unit cells in the 19 metal sheets used to create the BPF, as shown in Fig. 5. When stacking all layers together, the total thickness of the resulting MLW filter is less than 6 mm. The simulated performance of the MLW filter considering silver as building material is plotted in Fig. 6. In this result we have considered an air-

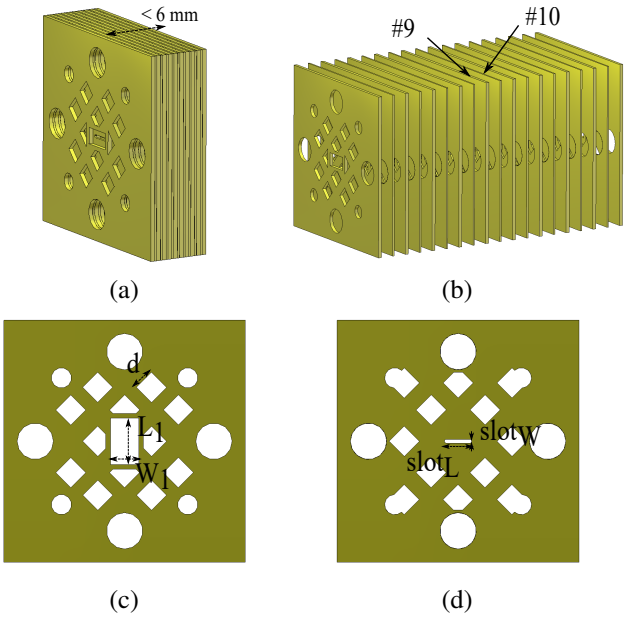

Fig. 5. The proposed multi-layer waveguide (MLW) BPF. (a) 3-D exploded view. (b) side view of layers. (c) details of layer 9. (d) details of layer 10.

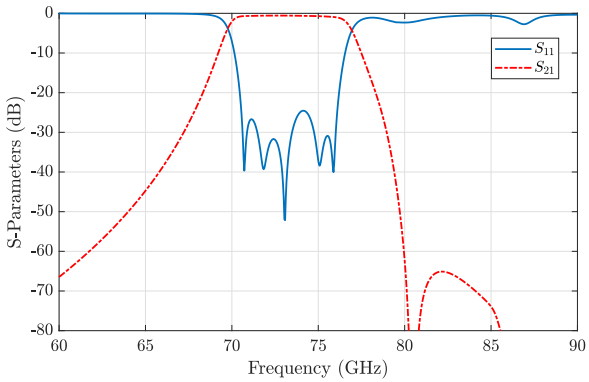

Fig. 6. Simulated performance of the designed MLW BPF.

gap of 10 μm between all neighboring layers. Fig. 6 shows a similar performance as the simple model of Fig. 2. The insertion loss is better than 0.9 dB between 71-76 GHz, and return loss is better than 24.5 dB in the same frequency band.

III. Experimental Validation

In this section, an experimental validation of the performance of the proposed E-band MLW filter is presented in terms of S-parameters and thermal sensitivity evaluation. The viability for mass-producing MLW components is also briefly discussed by describing the employed manufacturing method and the assembly process of the layers that we followed to build up the MLW filters.

A. Fabrication and assembly

A high-volume fabrication method and automatic assembly process have been followed and consists of three main steps:

metal panel fabrication, panel attachment/assembly and panel cutting for filter sample separation.

Each metal layer used to build up the whole MLW filter are made of silver-plated (5-7 μm plating) brass panels. The desired pattern on each layer are formed by using metal chemical etching. Chemical etching is a highly accurate manufacturing process that can produce very precise metal parts with any desired shape including complex geometries. This technique is suitable for large scale production due to the flexible and cost-effective employed etching tools and its shorter lead time. As it is explained in [16], the fabrication tolerance is around $\pm\ 10-20\%$ of the metal sheet thickness. This tolerance can be preliminary compensated in the design, thus reducing the final manufacturing errors.

A set of 19 panels (total number of layers of our filter) was fabricated. Each panel contains 12 rows and 18 columns of the corresponding pattern for each MLW filter layer, thereby resulting in a total of 216 filter samples. Fig. 7 illustrates a fabricated panel by metal chemical etching containing the corresponding pattern for one of the layers of the MLW filter. Each panel was placed in a fixture, and a dispenser machine was programmed to apply adhesive epoxy following a certain path around each sample (see Fig. 8). After securing and aligning all layers on the fixture, the panels were heated in an oven to cure the epoxy and achieve proper attachment. The fixture ensures that the alignment error between the layers remains below $\pm$ 50 μm, which is the maximun misalignment that we can accept according to our simulations.

The last step of the assembly procedure is to separate the 216 filter samples from each 19-layers panel. For this purpose waterjet cutting is used to cut out the filters.The final BPF samples are well defined and have very smooth side walls as can be observed in Fig. 9.

B. Experimental evaluation and thermal response

Cavity filters are known to be very sensitive to manufacturing tolerances and thermal variations, but the approach described in [18] to implement waveguide bandpass filters provides less sensitive configurations. The temperature dependence of the proposed MLW bandpass filter has been evaluated by using a thermal mini-chamber VT 4002, and Rohde&Schwarz ZVA-Z110E W-band extenders connected to a ZVA67 Vector Network Analyzer (VNA). The MLW

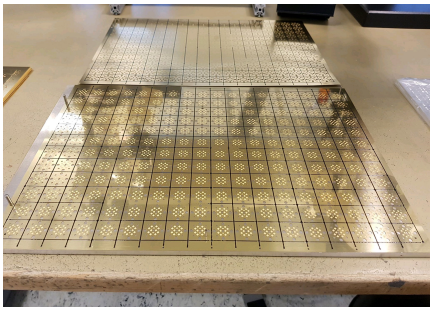

Fig. 7. Fabricated MLW panel secured on a fixture to ensure alignment.

Fig. 8. Machine dispensing epoxy around the MLW pattern in a certain panel.

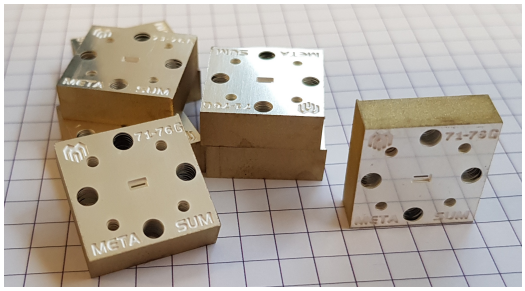

Fig. 9. Fabricated MLW filters after water-jet cutting.

filter thermal response has been compared with the thermal performance of a commercial E-band waveguide filter reported in [8]. Our measurement setup is illustrated in Fig. 10, and the measurements of the S-parameters for four temperature values in the range from -30°C to +70°C are plotted in Fig. 11. Table II shows a summary of the measured results including the center frequency thermal stability parameter δ_f (expressed in parts-per-million per degree Celsius) that gives an estimation of how stable the filter performance is in temperature variations. A low value of δ_f is desired since it indicates that the filter response shows a low frequency drift in different temperature scenarios. This parameter is calculated by using the formula [8]:

$$\delta_f = \frac{\Delta f}{\Delta T \cdot f_{T_0} \cdot 10^{-6}}. \tag{2}$$

where ΔT is the temperature variation, and Δf is the center frequency variation in the temperature range under study. The measured δ_f of the MLW filter over the entire temperature range from -30°C to +70°C is 9.3 ppm/°C, which outperforms commercial resonant cavity E-band waveguide filters as the one in [8] with center frequency thermal stability of 27.32 ppm/°C. The obtained relative center frequency shift over the whole temperature interval for our proposed MWL filter is 0.12%. When the temperature is +30°C, the measured insertion loss is better than 1.3 dB between 71.5-76 GHz, and return loss is better than 15 dB in the same frequency band.

IV. Conclusion

The design, implementation and experimental validation of an E-band bandpass filter developed in MLW technology has been presented in this paper. The obtained measurement results

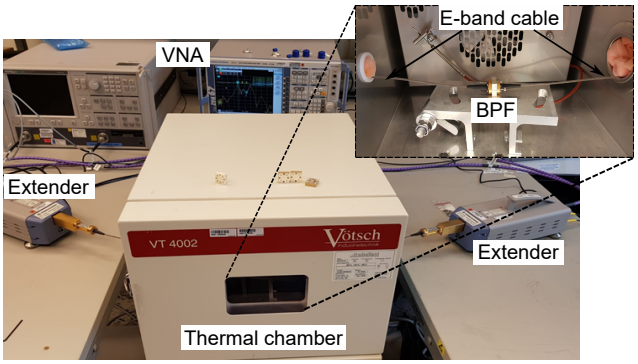

Fig. 10. Thermal measurement setup.

TABLE II
MEASURED THERMAL PERFORMANCE OF E-BAND MLW FILTER

Temperatures	-30°C	0°C	T_0= +30°C	+70°C
Center frequency (GHz)	74.54	74.51	74.47	74.45
-15 dB bandwidth (GHz)	5.97	5.92	5.91	6.01
$\|S_{11}\|$ (dB)	-17.9	-17.7	-17.84	-17.82
$\|S_{21}\|$ (dB)	-0.93	-0.91	-0.89	-0.89
Center frequency thermal stability, δ_f (ppm/°C)	9.3			
Relative center frequency shift, Δ_f (%)	0.12			

confirm the capability for realizing low loss and ultra-compact MLW filters in large volumes. Our thermal measurements show that the MLW filters are less sensitive to temperature variations than commercial E-band waveguide filters reported so far. We should remark that MLW is a flexible technology that can be applied for designing any type of passive component, antennas, and packaging of active circuits.

ACKNOWLEDGMENT

The authors would like to thank Tony Josefsson and Andreas Martin from Ericsson AB, Borås (Sweden), for their support related to the assembly process of MLW components.

REFERENCES

[1] F. C. Commission *et al.*, "Allocation and Service Rules for the 71-76 GHz, 81-86 GHz, and 92-95 GHz Bands," *FCC Memorandum Opinion and Order*, pp. 03–248, 2003.

[2] D. Lockie and D. Peck, "High-data-rate millimeter-wave radios," *IEEE Microw. Mag.*, vol. 10, no. 5, pp. 75–83, 2009, dio: 10.1109/MMM.2009.932834.

[3] J. Hansryd, Y. Li, J. Chen, and P. Ligander, "Long term path attenuation measurement of the 71–76 GHz band in a 70/80 GHz microwave link,," in *Proceedings of the Fourth European Conference on Antennas and Propagation*. IEEE, 2010, pp. 1–4.

[4] G. Cannone and M. Oldoni, "High-yield E-band diplexer for fixed radio point-to-point equipment," *International Journal of RF and Microwave Computer-Aided Engineering*, vol. 24, no. 4, pp. 508–512, 2014.

[5] J. R. Aitken and J. Hong, "Design of millimetre wave diplexers with relaxed fabrication tolerances," *IET Microwaves, Antennas & Propagation*, vol. 9, no. 8, pp. 802–807, 2015.

[6] F. Teberio, P. Soto, I. Arregui, T. Lopetegi, S. Cogollos, I. Arnedo, P. Martin-Iglesias, V. E. Boria, and M. A. Laso, "Waveguide bandpass filter with reduced sensitivity to fabrication tolerances for q-band payloads," in *2017 IEEE MTT-S International Microwave Symposium (IMS)*. IEEE, 2017, pp. 1464–1467.

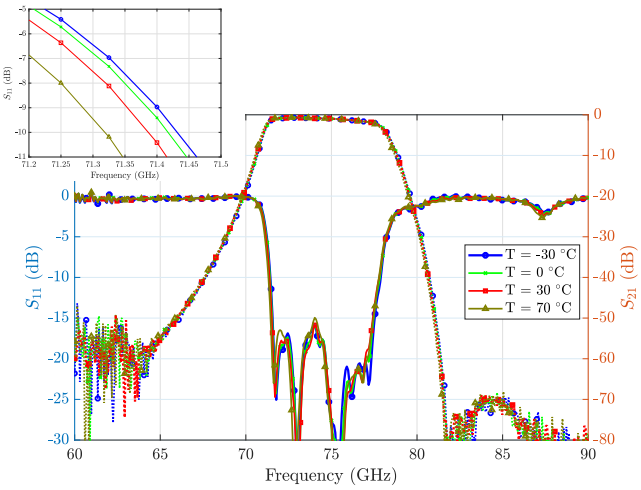

Fig. 11. Measured S-parameters of MLW filter for temperature range from -30°C to +70°C.

[7] T. Martin, A. Ghiotto, T.-P. Vuong, and F. Lotz, "Self-temperature-compensated air-filled substrate-integrated waveguide cavities and filters," *IEEE Transactions on Microwave Theory and Techniques*, vol. 66, no. 8, pp. 3611–3621, 2018.

[8] Y. Uemichi, O. Nukaga, X. Han, K. Kobayashi, S. Amakawa, and N. Guan, "Temperature dependence of bandpass filters built of silica-based post-wall waveguide for millimeter-wave applications," in *2018 48th European Microwave Conference (EuMC)*. IEEE, 2018, pp. 703–706.

[9] B. Zhang and H. Zirath, "Metallic 3-D printed rectangular waveguides for millimeter-wave applications," *IEEE Trans. Compon., Packag., Manuf. Technol.*, vol. 6, no. 5, pp. 796–804, 2016, doi: 10.1109/TCPMT.2016.2550483.

[10] X. Zhao, J. Bao, G. Shan, Y. Du, Y. Zheng, Y. Wen, and C. H. Shek, "D-band micromachined silicon rectangular waveguide filter," *IEEE Microw. Wireless Compon. Lett.*, vol. 22, no. 5, pp. 230–232, 2012, doi: 10.1109/LMWC.2012.2193121.

[11] X. Xu, M. Zhang, J. Hirokawa, and M. Ando, "E-band plate-laminated waveguide filters and their integration into a corporate-feed slot array antenna with diffusion bonding technology," *IEEE Transactions on Microwave Theory and Techniques*, vol. 64, no. 11, pp. 3592–3603, 2016.

[12] P.-S. Kildal, "Three metamaterial-based gap waveguides between parallel metal plates for mm/submm waves," *EuCAP 2009*, 2009.

[13] A. Vosoogh, M. S. Sorkherizi, V. Vassilev, A. U. Zaman, Z. S. He, J. Yang, A. A. Kishk, and H. Zirath, "Compact integrated full-duplex gap waveguide-based radio front end for multi-gbit/s point-to-point backhaul links at e-band," *IEEE Transactions on Microwave Theory and Techniques*, vol. 67, no. 9, pp. 3783–3797, 2019.

[14] X.-P. Chen and K. Wu, "Substrate integrated waveguide filter: Basic design rules and fundamental structure features," *IEEE Microwave Magazine*, vol. 15, no. 5, pp. 108–116, 2014.

[15] Y. Uemichi, O. Nukaga, K. Nakamura, X. Han, Y. Hasegawa, R. Hosono, K. Kobayashi, N. Guan, and S. Amakawa, "An E-band hybrid-coupled diplexer built of silica-based post-wall waveguide," in *2017 47th European Microwave Conference (EuMC)*. IEEE, 2017, pp. 819–822.

[16] A. Vosoogh, H. Zirath, and Z. S. He, "Novel air-filled waveguide transmission line based on multilayer thin metal plates," *IEEE Transactions on Terahertz Science and Technology*, vol. 9, no. 3, pp. 282–290, 2019.

[17] M. Ebrahimpouri, E. Rajo-Iglesias, Z. Sipus, and O. Quevedo-Teruel, "Cost-effective gap waveguide technology based on glide-symmetric holey EBG structures," *IEEE transactions on Microwave Theory and Techniques*, vol. 66, no. 2, pp. 927–934, 2017.

[18] F. Teberio, I. Arregui, P. Soto, M. A. Laso, V. E. Boria, and M. Guglielmi, "High-performance compact diplexers for Ku/K-band satellite applications," *IEEE Transactions on Microwave Theory and Techniques*, 2017.